Fluid Inclusion Study on the Moyoulete Sb-Cu Deposit, Xinjiang, China

Fluid Inclusion Study on the Moyoulete Sb-Cu Deposit, Xinjiang, China

Hui Zhang[1], Yinghua Zhang[1], Jiuhua Xu[1*], Xihui Cheng[2], Guorui Zhang[3] and Chunjing Bian[1]

[1] School of Civil and Resource Engineering, University of Science and Technology, Beijing, China

[2]MLR Key Laboratory of Metallogeny and Mineral Resources Assessment, Institute of Mineral Resources, CAGS, Beijing, China

[3]Center of Journals & Annals, Hebei GEO University, China

[*]Corresponding author's e-mail: jiuhuaxu@ces.ustb.edu.cn

Abstract. The Moyoulete Sb-Cu deposit occurs in Devonian Kelan volcanic-sedimentary basin, which strikes NW-SE along the south margin of Altay Mountains, hosted in lower Devonian upper kangbutiebao formation. Sulfide quartz veins could be divided into two stages: early stage (Q1), charactered by white lenticular or veinlet quartz veins of copper mineralization occurring in metamorphic crystal tuff, metamorphic basic volcanic rock, or rhyolite porphyry; late stage (Q2), charactered by copper-bearing grey-white pyrite-quartz veins cutting the metamorphic rocks. The four types of fluid inclusions in the quartz veins can be identified: 1) CO_2-rich fluid inclusions; 2) Water-rich fluid inclusions; 3) Carbonic fluid inclusions; 4) Aqueous fluid inclusions. CO_2-rich fluid inclusions in Q1 have $T_{m,CO2}$= -61.9~ -57.9 ℃ and $T_{h,CO2}$= -10.0~21.6 ℃; the $T_{h,tot}$s' are 358~388 ℃, while in Q2 have $T_{m,CO2}$= -63.2~ -60.2 ℃ and $T_{h,CO2}$= -20.4~17.4℃; the $T_{h,tot}$s' are 270~325℃ in the Moyoulete Sb-Cu deposit. The characteristics of CO_2-rich fluid inclusions from the Moyoulete Sb-Cu deposit are similar to those from other Cu-Au mineralization localities. The genesis of vein Sb-Cu mineralization was connected with the orogeny-metamorphism hydrothermal fluid, resulting from the orogeny metamorphism of the Late Permian-Triassic in the south margin of the Altay Mountains.

1. Introduction

The Moyoulete Sb-Cu deposit, located 15 km northwest to Altay (Figure 1), Xinjiang, occurs in Devonian Kelan volcanic-sedimentary basin, which strikes NW-SE along the south margin of Altay Mountains. Several Pb-Zn (Cu) and gold deposits have been studied for their geological characteristics, ore genesis, chronology, as well as fluid inclusions, such as the Tiemurte, the Dadonggou and the Sarekuobu [1-7]. However, the Moyoulete Sb-Cu deposit is merely confined to some descriptions about the geological characteristics, and no fluid inclusion study has been done as yet. Here we present the result of fluid inclusions in the Moyoulete Sb-Cu deposit and new insights of the ore genesis.

2. Regional geology

The Moyoulete Sb-Cu deposit is located in the Kelan Devonian–Carboniferous fore-arc basin and is hosted in Devonian volcanic-sedimentary strata (Figure 1). In the general deposit area, the Kelan basin consists of an overturned syncline that strikes 50 km, with the axial plane dipping to the northwest.

Rocks of the Silurian Kulumuti Group are exposed in the basement of the basin in the area and include migmatites, gneisses, and schists, which are unconformably overlain by the Devonian strata that include the Kangbutiebao and Altay Town Formations in the ascending sequence. The Early Devonian Kangbutiebao Formation is composed of metamorphosed intermediate-felsic lavas and pyroclastic rocks, and clastic and carbonate sediments. The Middle Devonian Altay Formation consists of slate, greywacke, schist, and phyllite. All the Devonian rocks were folded and metamorphosed to greenschist facies during the Hercynian Orogeny. Intermediate to felsic intrusions are widespread in the Altay orogenic belt, ranging from Ordovician, through Permian, to Triassic, and even to Early Jurassic in age.

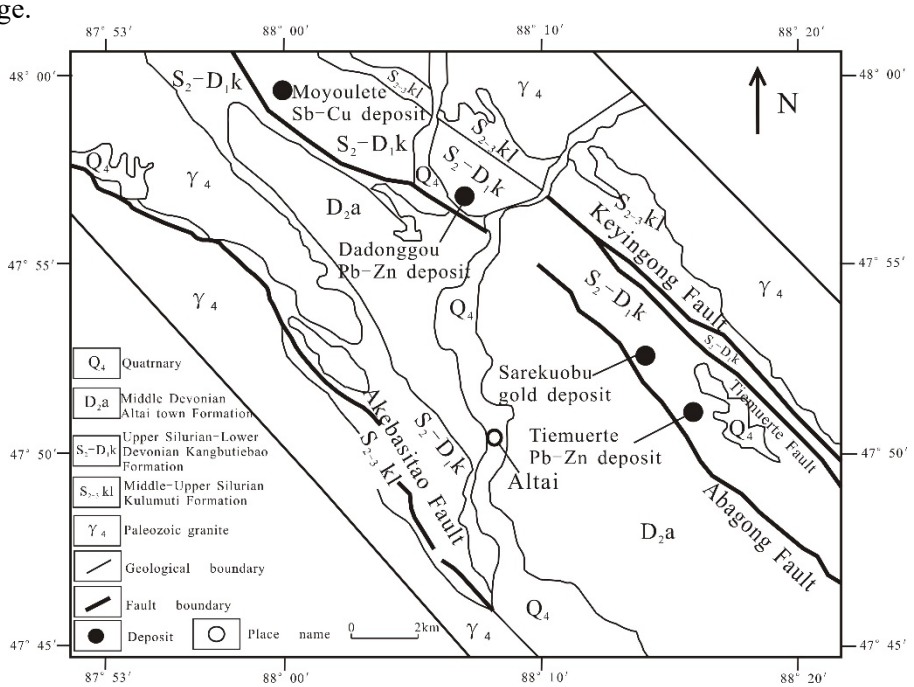

Figure 1. Geological map showing the regional geology and distribution of deposits in the Kelan basin, Altay [8,9]

Faults in the Kelan Basin are mainly NW-trending and are present as boundaries between terranes and between different stratigraphic units (Figure 1). The Keyingong (and Hongdun) faults divide the Silurian and Devonian strata, whereas the Abagong (and Altay) faults separate the Kangbutiebao and Altay Formations. The Abagong fault, as a subsidiary fault of the Erqis suture zone, controls the localization of the Dadonggou Pb–Zn deposit, the Tiemurt Pb–Zn–Cu deposit, and the Sarekuobu gold deposit, and shows conspicuous malachite staining. Some of these deposits, for example, Sarekuobu gold deposit and Tiemurt Pb–Zn–Cu deposit, have been recently considered as orogenic mineral systems [3,4].

3. Ore Geology

The Moyoulete Sb-Cu deposit, hosted in lower Devonian upper kangbutiebao formation composed of chlorite schist, metamorphosed calcareous sandstone and marble, not only is controlled by the stratigraphic horizons but by the regional Abagong-Kuerti fault as well. The deposit displays a strong correlation with the dacitic-rhyolitic volcanic rocks in this region. The ore bodies are mainly lenticular, stratoid or vein and the malachite mineralization is widespread in the surface. The main ore minerals are chalcopyrite, stibnite, pyrite, sphalerite and galena, with gangue minerals including quartz, chlorite, calcite and biotite. The wall rock alterations are mainly pyritization and sericitization.

Sulfide quartz veins could be divided into two stages: early stage (Q1), charactered by white lenticular or veinlet quartz veins of copper mineralization occurring in metamorphic crystal tuff,

metamorphic basic volcanic rock, or rhyolite porphyry; late stage (Q2), charactered by copper-bearing grey-white pyrite-quartz veins cutting the metamorphic rocks.

4. Fluid inclusions

The four types of fluid inclusions in the quartz veins can be identified: 1) CO_2-rich fluid inclusions (L_{CO2}-L_{H2O} type) (Figure 2), comprised of a liquid CO_2 and a liquid H_2O phases, with CO_2/H_2O volume ratio beyond 50% and 6~25 μm of sizes, mostly separately or in crowds distributes in Q1 and Q2 with different shapes such as ellipticity, elongation, or irregular shape. The remaining cavities can be seen owing to the fracture of fluid inclusions as a result of the tectonic deformation or late uplifting. Only a spot of homogenization temperature are acquired since the fluid inclusions burst as the pressure increased in the process of microthermometry; 2) Water-rich fluid inclusions (L_{H2O}-L_{CO2} type), comprised of a liquid H_2O phase and a liquid or vapour CO_2 phase, with CO_2/H_2O volume ratio less than 20% and sizes of 6~20 μm. mostly separately or in zonal distribute in Q1 and Q2 with different shapes; 3) Carbonic fluid inclusions ($L_{CO2\pm CH4\pm N2}$ type)(Figure 2), usually occurring as single phase at room temperatures, having 4~20 μm of sizes, mostly distributing in zonal or in crowds. Primary carbonic fluid inclusions in weakly deformed quartz Q2 around chalcopyrite grains were trapped during the mineralization period, while those crossing quartz grains show late structure-hydrothermal event; 4) Aqueous fluid inclusions (L_{H2O}-V_{H2O} type) (Figure 2), composed of a vapour and a liquid phase with 5 % to 30 % of V/L ratios and 5~15 μm of sizes. Most of them are secondary.

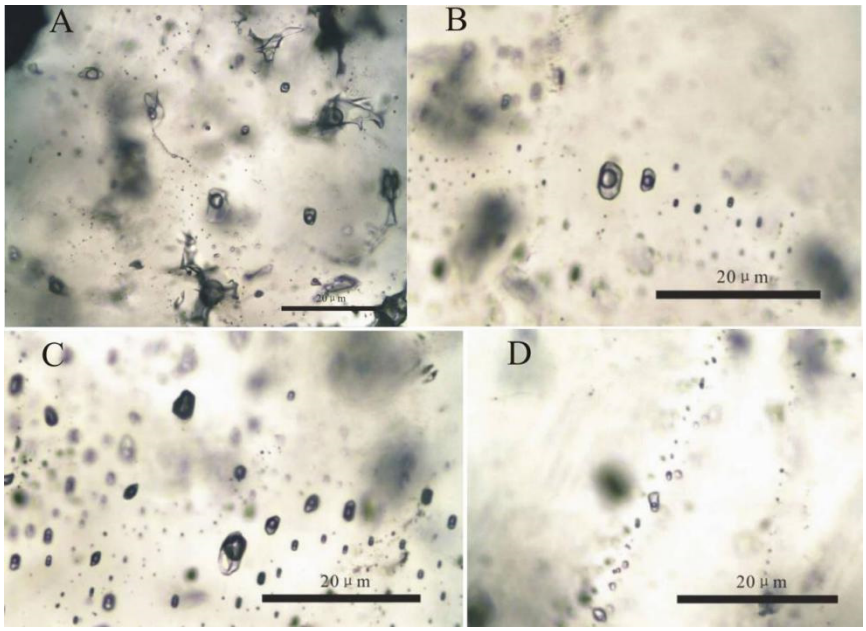

Figure 2. The characteristics of fluid inclusions from the Moyoulete Sb-Cu deposit

A and B-CO_2-rich fluid inclusions (L_{CO2}-L_{H2O} type); C-Carbonic fluid inclusions ($L_{CO2\pm CH4\pm N2}$ type); D-Aqueous fluid inclusions（L_{H2O}-V_{H2O} type）

On the whole, the early quartz veins (Q1) mainly contain the types of L_{CO2}-L_{H2O} and L_{H2O}-L_{CO2}, which distribute separately. It could be that the partial immiscibility of CO_2-H_2O resulting from the reduces of P-T occurred after the ore-forming fluids passed into the fracture dilatancy sites and resulted in the varieties of CO_2/H_2O volume ratio. The late quartz veins (Q2) contain a great deal of carbonic fluid inclusions and CO_2-rich fluid inclusions. Part of the primary carbonic fluid inclusions distributing separately or disorderly were trapped following the form of metamorphic hydrothermal quartz veins. Most of the secondary carbonic fluid inclusions distribute in groups or face shapes.

The results of microthermometry (Figure 3, Table 1) show that CO_2-rich inclusions in Q1 have $T_{m,CO2}$= -61.9~ -57.9 ℃ and $T_{h,CO2}$= -10.0~21.6 ℃, with X_{CH4}= 0.09~0.47 and ρ= 0.55~0.93 g/cm^3 on

the basis of V-X phase diagram and ρ-X_{CH4}-T_h diagram in the CO_2-CH_4 system[10-12]. Some inclusions containing much CH_4 or N_2 have $T_{m,CO2}$= -75.7~ -74.7 ℃ and $T_{h,CO2}$= -1.8~12.7℃. The total homogenization temperatures ($T_{h,tot}$) are 358~388 ℃(only a few data acquired). Carbonic fluid inclusions in Q1 have $T_{m,CO2}$= -58.5~ -58.4 ℃ and $T_{h,CO2}$= -10.1~12.0 ℃, with X_{CH4}= 0.16~0.28 and ρ= 0.60~0.88 g/cm^3. CO_2-rich fluid inclusions in Q2 have $T_{m,CO2}$= -63.2~ -60.2 ℃ and $T_{h,CO2}$= -20.4~17.4℃, with X_{CH4}= 0.18~0.57 and ρ= 0.50~0.95 g/cm^3. The $T_{h,tot}$s' are 270~325℃. Carbonic fluid inclusions in Q2 have $T_{m,CO2}$= -63.9~ -60.2 ℃and $T_{h,CO2}$= -47.6~20.5 ℃, with X_{CH4}= 0.18~0.78 and ρ= 0.55~1.21 g/cm^3. Raman spectra analysis of fluid inclusions shows that CO_2 phase in CO_2-rich inclusion of Q1 mainly contains CO_2, with small amount of N_2. Carbonic fluid inclusions of Q2 mainly contain CO_2, with certain amount of CH_4 and a spot of N_2. The results of Raman analysis are consistent with those of microthermometry.

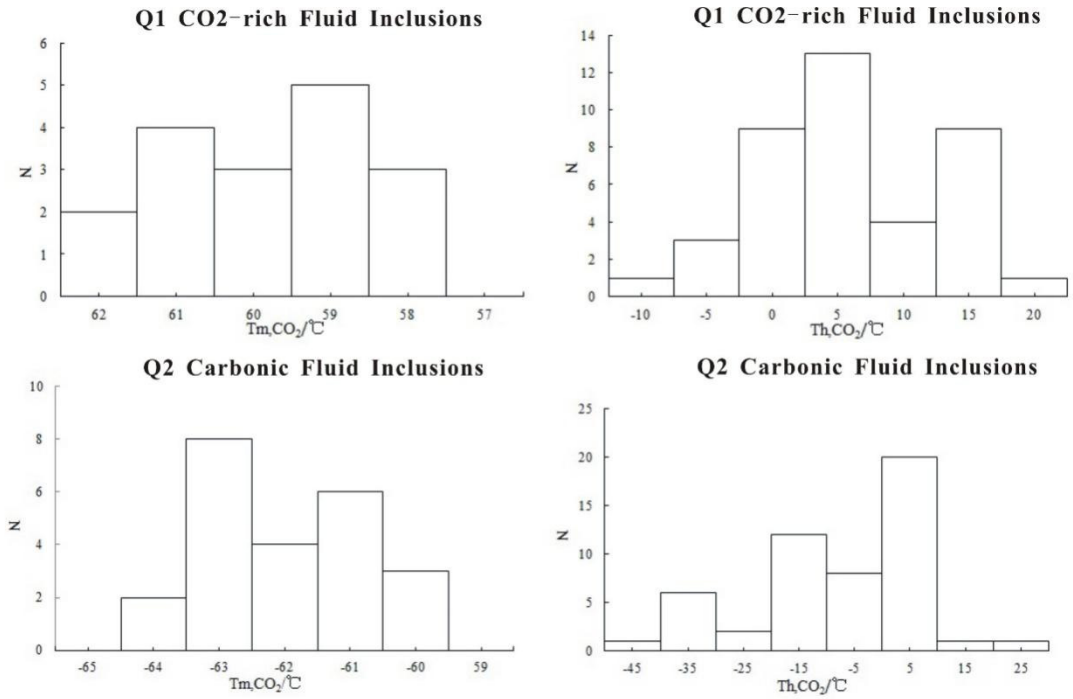

Figure 3. Microthermometry of CO_2 phase from the fluid inclusions of Moyoulete Sb-Cu deposit

Table 1. The results of microthermometry of fluid inclusions from Moyoulete

Stage	Type of FI	$T_{m,CO2}$(℃)	$T_{h,CO2}$(℃)	$T_{h,tot}$(℃)	$T_{e,CO2.nH2O}$(℃)	ρ(g·cm^{-3})
Q1	CO_2-rich FI	-61.9~-57.9	-10.0~21.6	358~388	0.4~7.9	0.55~0.93
Q1	Carbonic FI	-58.5~-58.4	-10.1~12.0			0.60~0.88
Q2	CO_2-rich FI	-63.2~-60.2	-20.4~17.4	270~325		0.50~0.95
Q2	Carbonic FI	-63.9~-60.2	-47.6~20.5			0.55~1.21

5. Trapping P-T conditions of fluid inclusions

The trapping pressures could be acquired by the method that the upper and lower limits of the CO_2 isochore in the P-T phase diagram from CO_2 fluid inclusion could be defined according to the ranges of $T_{h,CO2}$ from the carbonic fluid inclusions as well as the temperature ranges could be defined according to the ranges of $T_{h,tot}$ from the CO_2-rich fluid inclusions in the same sample [13]. The results show that the minimum trapping pressures of CO_2-rich metamorphic fluid in the Moyoulete Sb-Cu deposit vary from 150 to 433 MPa (Figure 4). These data are similar to the pressures for the Altay orogeny during ductile and brittle tectonic deformation (250 to 400 MPa) [14,15] and the minimum

trapping pressures of carbonic fluid inclusions in metamorphic sulfide quartz veins of the Tiemurte and Dadonggou Pb-Zn (Cu) deposits (120~340 MPa) [1].

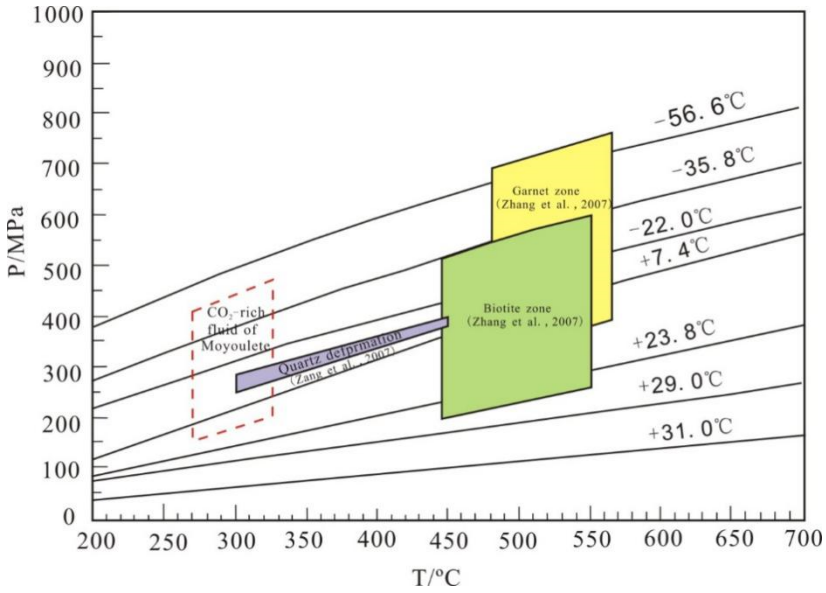

Figure 4. The pressure-temperature evolution path of the regional metamorphic belt on the southern margin of Altay, deformation quartz and CO_2-rich fluid inclusions in the metamorphism quartz veins from Moyoulete Sb-Cu deposit [13-15]

6. Conclusions

CO_2-rich fluid inclusions in Q1 have $T_{m,CO2}$= -61.9~ -57.9 ℃ and $T_{h,CO2}$= -10.0~21.6 ℃, the $T_{h,tot}$s' are 358~388 ℃, while in Q2 have $T_{m,CO2}$= -63.2~ -60.2 ℃ and $T_{h,CO2}$= -20.4~17.4℃, the $T_{h,tot}$s'are 270~325℃ in the Moyoulete Sb-Cu deposit. The characteristics of CO_2-rich fluid inclusions from the Moyoulete Sb-Cu deposit are similar to those from other Cu-Au mineralization localities. The genesis of vein Sb-Cu mineralization was connected with the orogeny-metamorphism hydrothermal fluid, resulting from the orogeny metamorphism of the Late Permian-Triassic in the south margin of the Altay Mountains.

Acknowledgements

This paper is funded by National Nature Science Foundation of China (41372096, 41672070). Thanks also to Prof. Fan HR of IGG-CAS for Raman analysis.

References

[1] Xu, J.H., Craig, H., Wang, L.L., Chu, H.X., Ding, R.F., Lin, L.H and Wei, X.F. (2011) Carbonic fluid overprints in volcanogenic massive sulfide deposits: examples from the Kelan volcano-sedimentary basin, Altaids, China. Economic Geology, 106: 145–158.

[2] Zheng, Y., Zhang, L.， Chen, Y.J., Qin, Y.J., and Liu, C.F. (2012) Geology, fluid inclusion geochemistry, and $^{40}Ar/^{39}Ar$ geochronology of the Wulasigou Cu deposit, and their implications for ore genesis, Altay, Xinjiang, China. Ore Geology Reviews, 49: 128–140.

[3] Zhang, L., Zheng, Y and Chen, Y.J. (2012) Ore geology and fluid inclusion geochemistry of the Tiemurt Pb–Zn–Cu deposit, Altay, Xinjiang, China: a case study of orogenic-type Pb–Zn systems. Journal of Asian Earth Sciences, 49: 69–79.

[4] Zhang, L., Chen, H.Y., Zheng, Y., Qin, Y.J. and Li, D.F. (2014) Geology, fluid inclusion and age constraints on the genesis of the Sarekuobu gold deposit in Altay, NW China. Geological Journal. DOI: 10.1002/gj.2573.

[5] Zheng, Y., Zhang, L. and Guo, Z.L. (2013) Zircon LA-ICP-MS U–Pb and biotite $^{40}Ar/^{39}Ar$ geochronology of the Tiemurt Pb–Zn–Cu deposit, Xinjiang: implications for the ore genesis. Acta Petrologica Sinica, 29: 191–204.
[6] Xu, J.H., Ding, R.F., Wei X.F., Zhong, C.H. and Shan, L.H. (2008) The source of hydrothermal fluids for Sarekuobu gold deposit in the southern Altai Mountains in Xinjiang, China: evidence from fluid inclusions and geochemistry. Journal of Asian Earth Sciences, 32: 247–258.
[7] Xu, J.H., Lin, L.H., Wang, L.L., Chu, H.X., Wei, X.F. and Chen, D.L. (2009) Defomation, metamorphism and carbonic fluids in VMS deposits of Kelan Basin, Altay. Mineral Deposits, 28(5): 585–598.
[8] Yin, Y.Q., Yang, Y.M., Li, J.X., Guo, Z.L. and Guo, X.J. (2005) Sediment-structural evolution and lead-zinc mineralization in the devonian volcano-sedimentary Kelan basin in Southern Altay, Xinjiang. Geotectonica et Metallongenia, 29(4): 475–481.
[9] Geng, X.X., Yang, J.M., Yao, F.J., Yang, F.Q., Liu, F and Chai, F.M. (2010) Ore-search information extraction from remote sensing data and integrated analysis of multiple geochemical information for the Abagong lean-zinc deposit in the Altay region, Xinjiang China. Geology and Exploration, 46(5): 942–952.
[10] Collins, P.L.F. (1979) Gas hydrates in CO_2-bearing fluid inclusions and the use of freezing data for estimation of salinity. Economic Geology, 74(6): 1435–1444.
[11] Swanenberg, H.E.C. (1979) Phase equilibria in carbonic systems and their application to freezing studies of fluid inclusions. Contributions to Mineralogy and Petrology, 68: 303–306.
[12] Thiery, R., Vidal, J., and Dubessy, J. (1994) Phase equilibria modeling applied to fluid inclusions: Liquid-vapour equilibria and calculation of the molar CO_2-CH_4-N_2 system. Geochimica et Cosmochimica Acta, 58(3): 1073–1082.
[13] Van den Kerkhof, A and Thiery, R. (2001) Carbonic inclusions. Lithos, 55: 49–68.
[14] Zang, W.S., Chen, B.L., Wu, G.G., Zhang, Z.C. and Yan, S.H. (2007) X-ray fabric analysis of deformed rocks inthe eastern part of the Fuyun-Qinghe area, Altay, Xinjiang, China. Geol. Bull. China, 26(9): 1189–1197.
[15] Zhang, C.G., Wei, C.J., Hou, R.S., Hou, L.S. and Pu, X.P. (2007) Phase equilibrium of low-pressure metamorphism in the Altaides, Xinjiang. Geology in China, 34 (1): 34–41.